

Thermal and Morphological Effects on the Hydrolytic Stability of Aluminum Tris(8-hydroxyquinoline) (Alq₃)

Keith A. Higginson, Xian-Man Zhang,[†] and Fotios Papadimitrakopoulos*

Department of Chemistry, Polymer Science Program, Institute of Materials Science, University of Connecticut, Storrs, Connecticut 06269-3136

Received July 25, 1997. Revised Manuscript Received January 12, 1998

An investigation into the physical and chemical characteristics of aluminum tris(8-hydroxyquinoline) (Alq₃), a reliable electron-transporting and emitting material for low molecular weight based organic light-emitting diodes (OLEDs), was performed. In the presence of atmospheric moisture, the thermal stability of Alq₃ was studied by monitoring the evolution of its volatile byproduct, 8-hydroxyquinoline (8-Hq), using thermogravimetric analysis and gas chromatography/mass spectroscopy (GC/MS). Sample morphology was shown to be an important parameter in the stability of Alq₃. Annealed (more crystalline) samples exhibited greater stability to hydrolysis than freshly sublimed films, at the expense of photoluminescence efficiency. The possible implications of these phenomena are discussed with respect to failure mechanisms of Alq₃-based OLEDs.

Introduction

Both low molecular weight and polymeric materials have been extensively investigated for use in organic light-emitting diodes (OLEDs) and related devices.¹ Sublimable organics are on the forefront of development due to their high attainable purity and flexibility in device fabrication.¹⁻³ The promise of high brilliance, cost-effective, flexible displays and illuminators has fueled progress in device optimization, such as color tuning, greater efficiencies, light outcoupling, and lifetime improvement.²⁻⁶ Unfortunately, low molecular weight organics undergo a number of morphological changes at elevated temperatures, which are deleterious to device performance.^{7,8} These mechanical relaxations can be slowed, primarily with the introduction of crystallization-resistant materials⁹⁻¹¹ or molecular dopants⁶ (which also improve emission efficiency and color tuning). Crystallization, however, is still difficult

to control over long time scales and may also, along with localized heating from uneven current distributions at film irregularities and ITO imperfections, facilitate a number of failure processes.^{3,4,12-14} At prolonged operation, the gradual electroluminescence (EL) decay and device resistance increase^{3,4} warrant investigation of typically slow processes, such as physical aging¹⁵ and chemical, photochemical, and/or electrochemical degradation.^{16,17}

Aluminum tris(8-hydroxyquinoline) (Alq₃) has risen to a prominent position in the development of robust OLEDs due to its relative stability as an electron-transporting and emitting material.^{2,3} The instability of this chelate in acidic environments is well-documented,¹⁸ and it has been recently shown to undergo a ligand-exchange reaction with water at elevated temperatures.^{19,20} Scheme 1 illustrates the oxyquinoline ligand being replaced by water, forming free 8-hydroxyquinoline (8-Hq) and other byproducts similar to those reported in the literature.^{21,22} The freed 8-Hq may then undergo further reactions to produce nonemissive species that can act as luminescence quenchers.¹⁹

* To whom correspondence should be addressed.

[†] Present address: Department of Chemistry, Wesleyan University, Middletown, CT 06459.

(1) Sheats, J. R.; Andoniadis, H.; Hueschen, M.; Leonard, W.; Miller, J.; Moon, R.; Roitman, D.; Stocking, A. *Science* **1996**, *273*, 884.

(2) Tang, C. W.; VanSlyke, S. A.; Chen, C. H. *J. Appl. Phys.* **1989**, *65*, 3610.

(3) Shi, J.; Tang, C. W. *J. Appl. Phys.* **1996**, *70*, 1665.

(4) VanSlyke, S. A.; Chen, C. H.; Tang, C. W. *Appl. Phys. Lett.* **1996**, *69*, 2160.

(5) VanSlyke, S. A.; Bryan, P. S.; Tang, C. W. *Proceedings of the Electroluminescence Workshop*, Wissenschaft and Technik: Berlin, 1996; p 195.

(6) Sano, T. *Proceedings of the Electroluminescence Workshop*, Wissenschaft and Technik: Berlin, 1996; p 196.

(7) Han, E.-M.; Do, L.-M.; Yamamoto, N.; Fujihira, M. *Thin Solid Films* **1996**, *273*, 202.

(8) Do, L.-M.; Han, E. M.; Nitedome, Y.; Fujihira, M.; Kanno, T.; Yoshida, S.; Maeda, A.; Ikushima, A. J. *J. Appl. Phys.* **1994**, *76*, 5118.

(9) Shirota, Y.; Kuwabara, Y.; Inada, H.; Wakimoto, T.; Nakada, H.; Yonemoto, Y.; Kawami, S.; Imai, K. *Appl. Phys. Lett.* **1994**, *65*, 807.

(10) Tanaka, H.; Tokito, S.; Taga, Y.; Okada, A. *Chem. Commun.* **1996**, 2175.

(11) Adachi, C.; Nagai, K.; Tamoto, N. *Appl. Phys. Lett.* **1995**, *68*, 2697.

(12) McElvain, J.; Andoniadis, H.; Hueschen, M.; Miller, J.; Roitman, D.; Sheats, J.; Moon, R. *J. Appl. Phys.* **1996**, *80*, 6002.

(13) Antoniadis, H.; Hueschen, M. R.; McElvain, J.; Miller, J. N.; Moon, R. L.; Roitman, D. B.; Sheats, J. R. *ACS Polym. Prepr.* **1997**, *38*, 382.

(14) Burrows, P. E.; Bulovic, V.; Forrest, S. R.; Sapochak, L. S.; McCarthy, D. M.; Thompson, M. E. *Appl. Phys. Lett.* **1994**, *65*, 2922.

(15) Thomsen, D. L.; Phely-Bobin, T.; Papadimitrakopoulos, F. *Mater. Res. Soc. Symp. Ser.*, in press.

(16) Papadimitrakopoulos, F.; Yang, M.; Rothberg, L. J.; Katz, H. E.; Chandross, E. A.; Galvin, M. E. *Mol. Cryst. Liq. Cryst.* **1994**, *256*, 663.

(17) Chadha, S. S. In *Solid State Luminescence*; Kitai, A. H., Ed.; Chapman & Hall: New York, 1993; p 159.

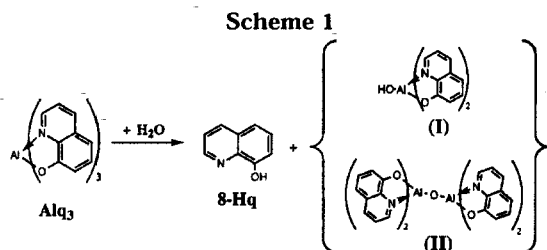
(18) Phillips, J. P. *Chem. Rev.* **1956**, *56*, 271.

(19) Papadimitrakopoulos, F.; Zhang, X.-M.; Thomsen, D. L.; Higginson, K. A. *Chem. Mater.* **1996**, *8*, 1363.

(20) Papadimitrakopoulos, F.; Zhang, X.-M. *Synth. Met.* **1997**, *85*, 1221.

(21) Scherer, P. R.; Fernando, Q. *J. Anal. Chem.* **1968**, *40*, 1938.

(22) Kushi, Y.; Fernando, Q. *J. Am. Chem. Soc.* **1970**, *92*, 91.



This paper discusses the temperature stability and sample morphology of sublimed Alq_3 films and bulk material. Increasing the crystallinity of Alq_3 films resulted in improved hydrolytic stability, although accompanied by decreased photoluminescence efficiency.

Experimental Section

Alq_3 was synthesized according to the literature method and purified twice by sublimation,¹⁹ stored in a nitrogen drybox, and transferred with as little atmospheric exposure as possible. Alq_3 films of several micrometers were evaporated at 7–10 Å/s on glass slides (cleaned with 7:3 $\text{H}_2\text{SO}_4/\text{H}_2\text{O}_2$, rinsed with deionized water, and dried with compressed air) at room temperature.

X-ray diffraction (XRD) was performed on a Norelco/Phillips diffractometer using $\text{Cu K}\alpha$ radiation ($\lambda = 1.5418 \text{ \AA}$). Thick Alq_3 films (several millimeters) were evaporated on glass slides for measurement of their XRD spectra before and after annealing, followed by subtraction of the substrate background. The film was annealed at 200 °C in a vacuum oven (1×10^{-5} Torr) equipped with a liquid nitrogen trap to prevent contamination by diffusion pump oil.

Differential scanning calorimetric (DSC) measurements at 10 °C/min scanning rate were conducted with a Perkin-Elmer DSC-7, employing a 20 mL/min flow of dry nitrogen as a purge gas for the sample and reference cells. The DSC temperature and power ordinates were calibrated with the melting point and heat of fusion of high-purity indium. In a nitrogen drybox, about 10 mg of sublimed or annealed Alq_3 was scraped from its substrate, packed into the DSC pan, and compression sealed with a Perkin-Elmer crimper press to prevent moisture contamination while transferring to the DSC, as well as to provide good thermal contact with the DSC pan.

A Perkin-Elmer TGA-7 was used for the thermogravimetric analysis (TGA) at a scan rate of 10 °C/min. A 10 mL/min flow of dry nitrogen was used to purge the sample at all times.

A Hewlett-Packard 5985 GC/MS equipped with a direct dynamic headspace injector (DDHI, a specialized accessory used for the analysis of volatile materials formed from nonvolatile solids^{20,23}) was used to study the degradation reaction. The DDHI allows automatic transfer to and from the GC injection port. Alq_3 samples (10–20 mg, powder or evaporated films, ca. 1000 Å on aluminum foil) were placed in small glass tubes, exposed to moisture, and placed in the DDHI, using a new sample each time. During the entire course of the measurement, the sample remains under high-purity helium. The column used was OV-1 fused silica capillary column 0.32 mm \times 50 m, 1.2 mm in size. The injection port temperature was varied to probe the temperature dependence of the reaction, and the samples were normalized with respect to their initial masses. The chromatography was carried out by temperature programming at 15 °C/min rate, from 35 to 300 °C. The mass spectroscopy had a range of 10–1000 atomic mass units. Electron impact ionization was used at 70 eV, and the scanning rate was 400 atomic amu/s.

Photoluminescence (PL) spectra were obtained with a Perkin-Elmer LS50B luminescence spectrometer. A special cuvette was fabricated which could be evacuated to approxi-

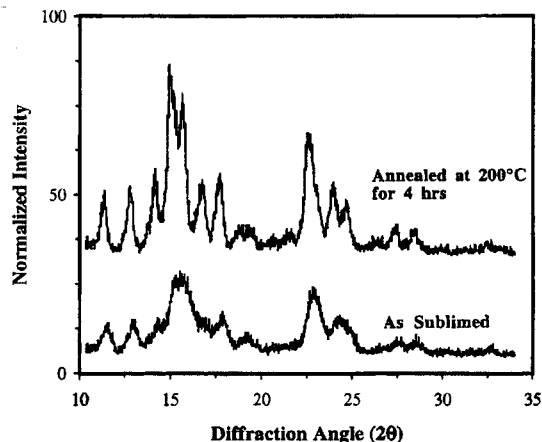


Figure 1. XRD spectrum of freshly sublimed and annealed Alq_3 samples.

mately 8×10^{-6} Torr and flame sealed. 1000 Å of Alq_3 was evaporated on a glass slide, followed by 1000 Å of magnesium, and secured within the cuvette. The films were annealed at 175 °C by placing the entire cuvette in a constant-temperature bath. Reflection UV-vis spectra were collected on a Perkin-Elmer Lambda 3840 array spectrophotometer after each annealing period to verify a constant optical density of the sample.

Results and Discussion

Tang et al.²⁴ have reported that sublimed films of Alq_3 exhibit a microcrystalline morphology with an average grain size of about 500 Å. This is in good agreement with the X-ray diffraction pattern of sublimed Alq_3 shown in Figure 1. Subjecting the same sample to 4 h annealing at 200 °C enhanced the intensity and narrowed the width of the diffraction peaks, indicating an increase in both crystal size and overall degree of crystallinity. Parameters such as the rate of deposition, substrate temperature, and surface treatment are likely to control both crystallite size and the phase distribution in such films.

Figure 2 shows the DSC traces (at 10 °C/min) for samples of freshly sublimed Alq_3 and those annealed for 2 h at 200 °C. The difference between the first heating scan of the freshly sublimed sample and all other scans is indicative of the amount of free volume present. The rather "noise-reminiscent" exotherms are not artifacts due to sample preparation or poor sample packing in the DSC pan but are quite reproducible, although the specific temperatures at which they occur vary from sample to sample. The rapid sorption of atmospheric moisture²⁵ will cause these peaks to disappear, probably due to a plasticization effect. These exotherms are usually observed above 125 °C, and their magnitude increases dramatically above 165 °C, past the first observable step change in heat capacity, usually associated with the glass transition temperature (T_g). The increased molecular mobility above T_g , in conjunction with the XRD data of Figure 1, suggests that these exotherms are due to sample crystallization. Subsequent heating and cooling scans show the absence of these exotherms and the appearance of a broad, fea-

(24) Tang, C. W.; VanSlyke, S. A. *Appl. Phys. Lett.* **1987**, *51*, 913.

(25) Papadimitrakopoulos, F.; Zhang, X.-M. *Synth. Met.* **1997**, *85*, 1221.

(23) Ezrin, M.; Lavigne, G. *SPE-ANTEC Proc.* **1991**, 2230.

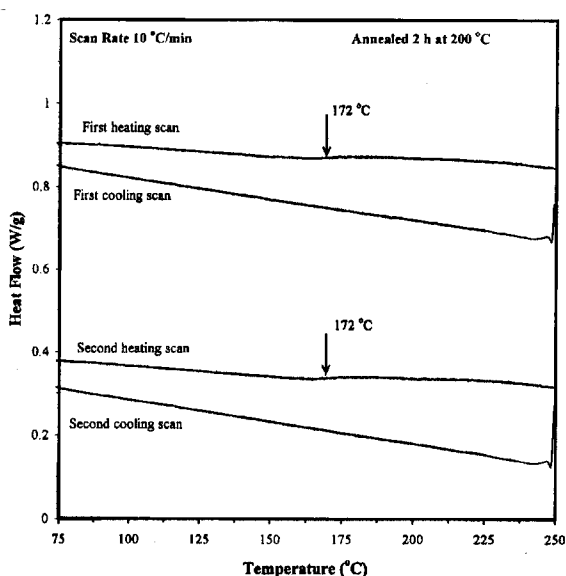
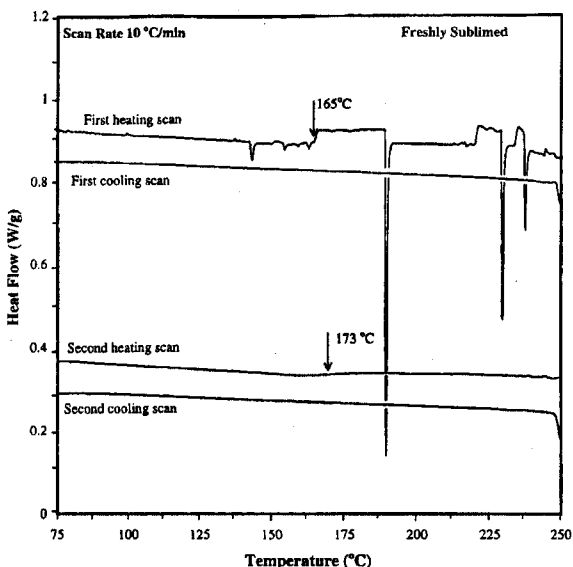


Figure 2. DSC traces for (A, top) freshly sublimed and (B, bottom) annealed Alq₃ samples.

tureless T_g (at about 172 °C), typical of a semicrystalline glass with a broad spectrum of relaxation times. The first heating scan of annealed Alq₃ (Figure 2B), which was prepared in the same fashion as the freshly sublimed sample, exhibited none of the crystallization exotherms seen in Figure 2A. This supports our conclusion that the exotherms are due to crystallization and not due to extrinsic effects such as sample rearrangement, etc., and demonstrates the irreversibility of this process in this temperature range.

Figure 3 shows the thermogravimetric analysis (TGA) of Alq₃ as a function of moisture content and morphology. Freshly sublimed and annealed samples (Figure 3B,C) show negligible weight loss (less than 0.02%) in the temperature range where the DSC measurements were conducted (see Figure 3, inset). Above 300 °C these two curves start to diverge, suggesting a slightly greater thermal stability for the annealed Alq₃ sample. Unsublimed samples, on the other hand, degrade rap-

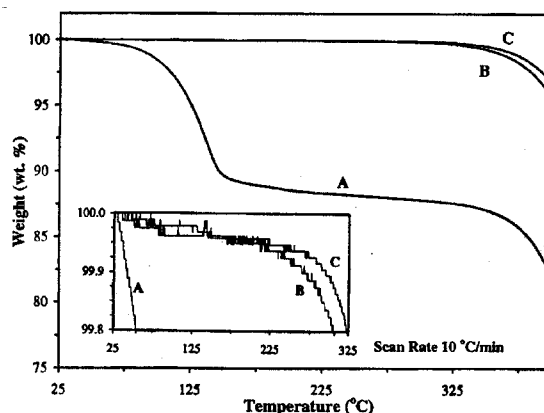


Figure 3. TGA traces for (A) nonsublimed, (B) freshly sublimed, and (C) annealed at 200 °C for 2 h Alq₃ samples.

idly at temperatures above 90 °C (Figure 3A), although the weight loss is evident at much lower temperatures (see Figure 3, inset). As has been verified by GC-MS (see following paragraphs), this decomposition is attributed to the loss of the volatile 8-hydroxyquinoline (8-Hq) ligand in the presence of water,^{19,20} which is nearly absent in the freshly processed samples. The cessation of the decomposition occurs as most of the absorbed water is spent (about 1.3 wt % by this measurement, assuming that 1 equiv of H₂O produces 1 equiv of 8-Hq). At temperatures greater than 250 °C, the weight loss is probably due to the unassisted thermolysis of the chelate or simply its sublimation.

Gas chromatography was used to quantitatively analyze the temperature dependence of the decomposition reaction in Scheme 1. Brief atmospheric exposure (several minutes) has been shown to be sufficient to produce detectable amounts of 8-Hq from Alq₃ samples.²⁰ Freshly sublimed Alq₃ powders or thin films were exposed to ambient moisture, and the chemical reaction was probed with GC. Significant amounts of 8-Hq were detected when the temperature of the injection port was set above 90 °C. Water was virtually absent from the GC trace, leaving 8-Hq as the only volatile compound detected in this temperature range. For a fixed injection time, the area of the 8-Hq elution peak (of roughly 15 s width) was normalized with respect to the initial sample mass and used to quantify the extent of reaction as a function of temperature. Care was taken to conduct these studies below the measured glass transitions in order to avoid the rapid morphological changes witnessed in Figure 2 and to limit the injection time so that only a fraction of the water is consumed.

Annealed Alq₃ showed a greater resistance to hydrolysis than the unannealed samples. The activation energy from the Arrhenius fits can be used to compare the thermal stabilities of both samples (see inset in Figure 4). The difference in activation energy is probably a result of the difference in free volume between the two sample morphologies. This would be reflected in both water diffusivity and the amount of amorphous Alq₃ participating in this reaction, since the material within the crystallites is comparatively inaccessible to moisture.²⁶

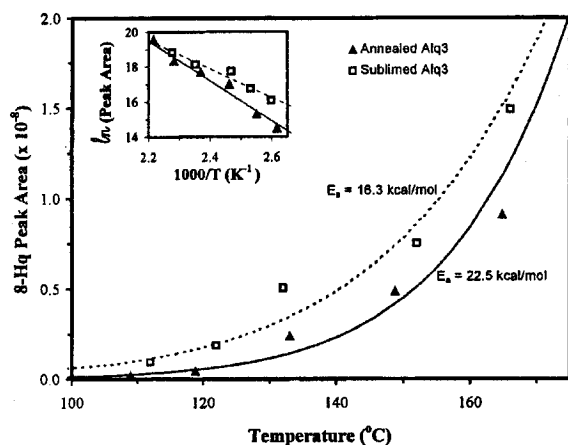


Figure 4. Evolution of 8-Hq as a function of temperature for freshly sublimed (unfilled squares) and 2 h, 200 °C annealed (filled triangles) Alq₃, as measured by GC-MS. Dashed and solid lines are Arrhenius fits to the data.

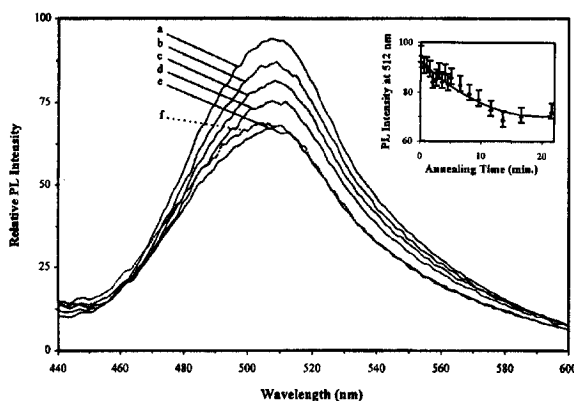


Figure 5. Photoluminescence spectra of a 1000 Å Alq₃ film at 175 °C under 8×10^{-6} Torr at (a) 0, (b) 3, (c) 6.5, (d) 9.5, (e) 16.5, and (f) 21.5 min annealing times. Inset plots the intensity at 512 nm as a function of annealing time.

Figure 5 shows the effect of annealing on the photoluminescence (PL) of 1000 Å Alq₃ films overcoated with 1000 Å Mg. Annealing these films at 175 °C, slightly above their T_g , resulted in a decrease of PL intensity. This was also accompanied by a slight red shift of the emission peak (507 nm at 0 min to 509 nm at 13.5 min). Both the PL decrease and red shift may be explained by the formation of aggregates or crystals which promote formation of excimers² or ground-state complexes. As the crystals get larger, however, an apparent increase in intensity and spectral blue shift is observed. This is not due to change of the emission characteristics but rather to the efficient Rayleigh scattering for shorter wavelengths (see Figure 5f), which was also accompanied by a visible roughening of the film.

The morphological characteristics of Alq₃ may contribute to three possible failure modes of its OLEDs: dimensional instability, luminance decay, and uneven charge transport.

The substantial volume shrinkage resulting from crystallization could create thickness irregularities in molecular sublimed thin films⁷⁻⁹ that lead to a large variation of the electric field for a given applied voltage

across the device. This could assist in the formation of high-current hot spots (similar to those observed from pinholes and ITO asperities^{8,12-14,27,28}) and eventually lead to dielectric breakdown, local short circuits in which the cathode penetrates the organics and contacts the ITO. Alternatively, the electrode may delaminate from the receding organic layer, possibly in conjunction with the loss of adhesion caused by water-assisted cathode oxidation^{12,13,28} or production of volatile products upon chemical decomposition.^{20,27}

The observed luminance decay of Alq₃ devices can be slowed with molecular doping,^{2,3,5} which may suppress crystallinity or contain the emission on localized, high-efficiency chromophores. In the cases where Alq₃ is the sole emitter, long-lived devices exhibit gradual luminance decay and corresponding increase in device resistance.⁴ Although an OLED is far more complex than the simple emission decay observed in Figure 5, the fact that the decay rate observed in devices is proportional to the current density supports the theory of Alq₃ crystallization. However, the intrinsic degradation of the Alq₃ chromophore, layer interdiffusion, contamination from ITO, and crystallization of hole-transport materials likely cause similar effects.

The increased charge mobility observed in organic crystals might also play an important role in contributing to uneven charge transport.^{29,30} In newly fabricated devices, the crystalline domains are surrounded by an amorphous matrix, maintaining uniform charge transport. The continued growth of crystals, however, at the expense of the amorphous region during prolonged device operation may increase the number of grain boundaries (which localize traps, impurities, and voids), and/or lead to preferential conduction pathways. Significant work is still needed to identify the different mechanisms and more explicitly relate them to the causes of device failure.

Conclusions

The hydrolytic stability of Alq₃ was discussed in light of temperature and morphology. Samples of higher crystallinity were found to be less susceptible to chemical attack by moisture, although they exhibited lower photoluminescence efficiency. The ramifications of these findings were discussed with respect to potential modes of device failure. The witnessed chemical and morphological transformations below the glass transition temperature of Alq₃ (ca. 172 °C) show the importance of these effects during prolonged, low-temperature device operation.

Acknowledgment. This research was financially supported by the Institute of Materials Science, Critical Technology Program, and by a Hewlett-Packard Fellowship to K.A.H. The authors wish to thank Mr. G. Lavigne and Dr. D. E. Bhagwagar for their expert technical assistance and Dr. H. Antoniadis for helpful discussions.

CM970599A

(27) Fujihira, M.; Do, L.-M.; Koike, A.; Han, E.-M. *Appl. Phys. Lett.* **1996**, *68*, 1787.

(28) Do, L.-M.; Oyama, M.; Koike, A.; Han, E.-M.; Yamamoto, N.; Fujihira, M. *Thin Solid Films* **1996**, *273*, 209.

(29) Garnier, F.; Peng, F. Z.; Horowitz, G.; Fichou, D. *Adv. Mater.* **1990**, *2*, 592.

(30) Dodabalapur, A.; Torsi, L.; Katz, H. E. *Science* **1995**, *268*, 270.

(26) Yeh, Y. S. *J. Polym. Sci.* **1990**, *28*, 545.